

Performance of p- and n-side illuminated microcrystalline silicon solar cells following 2 MeV electron bombardment

V. Smirnov, O. Astakhov, R. Carius, B. E. Pieters, Yu. Petrusenko, V. Borysenko, and F. Finger

Citation: *Appl. Phys. Lett.* **101**, 143903 (2012);

View online: <https://doi.org/10.1063/1.4756907>

View Table of Contents: <http://aip.scitation.org/toc/apl/101/14>

Published by the [American Institute of Physics](#)



SciLight

Sharp, quick summaries **illuminating**
the latest physics research

Sign up for **FREE!**



Performance of p- and n-side illuminated microcrystalline silicon solar cells following 2 MeV electron bombardment

V. Smirnov,^{1,a)} O. Astakhov,¹ R. Carius,¹ B. E. Pieters,¹ Yu. Petrusenko,² V. Borysenko,² and F. Finger¹

¹*IEK-5 Photovoltaik, Forschungszentrum Jülich GmbH, Jülich, Germany*

²*National Science Center, Kharkov Institute of Physics and Technology, CYCLOTRON Facility, Kharkov, Ukraine*

(Received 26 July 2012; accepted 17 September 2012; published online 3 October 2012; corrected 5 October 2012)

The impact of defects on the performance of p- and n-side illuminated microcrystalline silicon solar cells is investigated. The absorber layer spin density N_S is controlled over some two orders of magnitude by electron bombardment and subsequent annealing steps. At increased N_S (between 3×10^{16} and 10^{18} cm^{-3}), performance of n-side illuminated cells is much more strongly reduced relative to p-side illuminated cells, particularly with regard to short circuit current density. Quantum efficiency measurements indicate a corresponding strong asymmetry in wavelength-dependence, which has been successfully reproduced by numerical device simulations. © 2012 American Institute of Physics. [<http://dx.doi.org/10.1063/1.4756907>]

The electronic quality of the absorber layer critically affects the performance of thin film silicon solar cells. In general, an increase in the number of defects in the absorber layer, such as dangling bonds, impairs the extraction of the photo-generated charge carriers and therefore reduces the photovoltaic performance of a solar cell. These defects can act as recombination centers, influencing the electronic transport of electron and holes and thereby the collection efficiency. Solar cells with amorphous silicon (a-Si:H) absorber layers are illuminated through the p-side for optimum stabilized performance. In the common view, this is the optimum configuration as the hole mobility is much lower than the electron mobility, and, furthermore, space charge arising from charged ambipolar defects gives rise to a low electric field in a large part of the intrinsic layer. The latter is particularly relevant for the degraded state, where the defect density is high.^{1–3} In contrast, it was reported that solar cells with microcrystalline silicon ($\mu\text{c-Si:H}$) absorber layers can be illuminated from either p- or n-side without any significant impact on their performance.⁴ It was suggested that in such case, the electron and hole mobility-lifetime products are both larger and more symmetrical than those found in amorphous silicon materials.^{4,5} The possibility to illuminate the cell with $\mu\text{c-Si:H}$ absorber from n-side was successfully explored by applying highly transparent n-type alloys, such as SiC ⁶ or SiO_x ⁷ as window layers. The reported high short circuit current densities above of 25 mA/cm^2 for $1 \mu\text{m}$ thick solar cells exceed the typical J_{sc} values obtained in p-side illuminated $\mu\text{c-Si:H}$ solar cells.

The comparison of the performance of p- and n-side illuminated solar cells can provide additional information on the electronic properties of the absorber layer material and principles of the device operation. In the present report, we focus on the impact of defects on the performance of p- and n-side illuminated $\mu\text{c-Si:H}$ solar cells. This is of interest for the fundamental understanding of the device physics, as well as

relevant for possible industrial applications, where an increased deposition rate may lead to the reduction in material quality and thus device performance.⁸ The results of this study are also important to evaluate the potential for the improvement in the performance of solar cells, if the absorber layer defect density is further reduced.

In our previous work,^{9,10} we have shown that 2 MeV electron bombardment combined with stepwise annealing may be used to vary the defect density of the absorber layer in p-side illuminated thin film solar cells over several orders of magnitude in a particular device, which, in the case of $\mu\text{c-Si:H}$, is not achievable with light-soaking. The here applied high energy electron bombardment at low temperatures leads to a spatially homogeneous increase in the defect density. Furthermore, the created defects can be annealed out at temperatures below the deposition temperature.¹¹ We have shown before⁹ that although every layer of the solar cell is exposed to the MeV electron beam, the dose of irradiation only has a noticeable influence on the absorber layer. In the present work, we show that while the “initial” ($N_S = 7 \times 10^{15} \text{ cm}^{-3}$) performance of p- and n-side illuminated cells is quite similar, it is dramatically reduced, most strongly in J_{sc} , in the case of n-side illuminated devices when the defect density of the absorber layer is increased. We performed numerical device simulations, demonstrating that the known difference in electron and hole mobilities alone cannot explain the observed asymmetry between p- and n-side illuminated cells. However, we found that the observed asymmetry is reproduced in simulations if the mean energy of the defect distribution is placed slightly above the mid-gap, which results in different electric field strengths at p-i and n-i interfaces. The asymmetric electric field distribution makes the case of p-side illumination more favorable for separation of excess charge carriers.

In the present work, both p-side and n-side illuminated single junction $\mu\text{c-Si:H}$ solar cells were prepared in substrate configuration,¹² i.e., in the n-i-p or p-i-n deposition sequence, respectively, and illuminated from the film side. The nominal thickness of the absorber layers was $1 \mu\text{m}$. Doped and intrinsic

^{a)}E-mail: v.smirnov@fz-juelich.de.

thin film silicon layers were prepared by PECVD using optimized standard deposition conditions and deposited directly on transparent conducting oxide (TCO), so no metal back reflector was used. The crystallinity of $\mu\text{c-Si:H}$ absorber layers, evaluated from Raman measurements, is around 70%. The performance of the cells has been investigated by current/voltage (J - V) measurements in dark and under AM 1.5 illumination and external quantum efficiency (EQE) measurements. In order to correlate the variations in the device parameters with defect density in the absorber layer, we measured electron spin resonance (ESR) on intrinsic $\mu\text{c-Si:H}$. For the ESR measurements, we use $\mu\text{c-Si:H}$ powder samples, deposited under identical deposition conditions to the absorber layers in solar cells.¹¹ Subsequently, both solar cells and intrinsic material (ESR samples) were treated with identical irradiation-annealing procedure, enabling a variation in the spin density N_s of over 2 orders of magnitude, between $7 \times 10^{15} \dots 10^{18} \text{ cm}^{-3}$. Additional experimental details can be found elsewhere.^{9,10}

Fig. 1 summarizes J - V characteristics of p-side and n-side illuminated $\mu\text{c-Si:H}$ solar cells, as a function of N_s , varied between 7×10^{15} to $1.3 \times 10^{18} \text{ cm}^{-3}$. It can be seen that both types of solar cells show reduction in all J - V parameters (η , V_{oc} , FF , and J_{sc}) with increased N_s . Much stronger degradation is evident for n-side illuminated cells: the open circuit voltage V_{oc} is reduced from 520 mV down to around 275 mV and 142 mV (by around 50% and 72%) in the case of p-side and n-side illuminated cells, respectively, when the N_s increases from 7×10^{15} up to $1.3 \times 10^{18} \text{ cm}^{-3}$. Over this range of N_s , the FF is reduced by 24% and 48% in the case of p-side and n-side illuminated cells, respectively. The strongest effects are observed in J_{sc} , which is reduced roughly 4 times in the case of p-side illuminated cell and 40 times in the case of n-side illumination (from 14 mA/cm^2 down to the 0.35 mA/cm^2 in the later case). We note that since no metal back reflector was used in the cells, the initial cell efficiencies have relatively low values originating from reduced short circuit current density J_{sc} . As a matter of speculation, extrapolation of our results suggests prospects of higher efficiency of microcrystalline silicon solar cells pro-

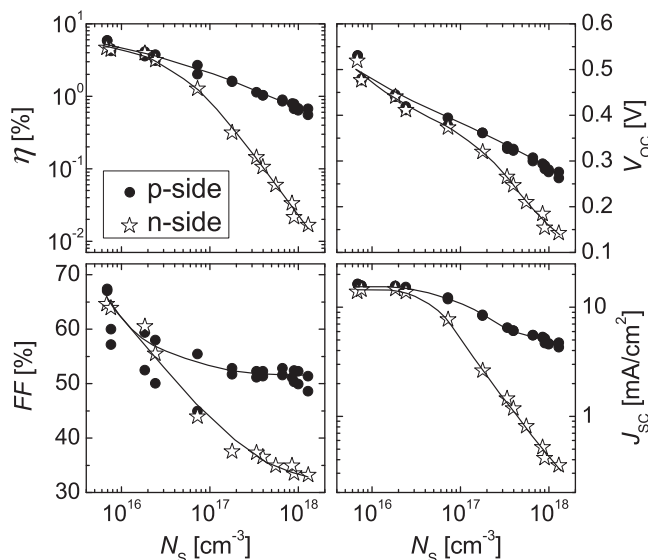


FIG. 1. J - V characteristics of p-side and n-side illuminated $\mu\text{c-Si:H}$ solar cells, plotted as a function of N_s . The lines are to guide the eye.

vided the absorber layer defect density is reduced below $N_s = 5 \times 10^{15} \text{ cm}^{-3}$.

The effects of defects on the short circuit current were further investigated with EQE measurements. The results are presented for p-side and n-side illuminated $\mu\text{c-Si:H}$ solar cells in Fig. 2. For the p-side illuminated solar cell, a reduction of EQE is observed in the longer wavelength part of the spectrum, while the EQE curves at $\lambda < 400 \text{ nm}$ are not affected by changes in N_s . This is in agreement with our previous observations.⁹ The picture is qualitatively different for the n-side illuminated solar cell: an increase in the absorber layer N_s results in the reduction of the EQE curves over the entire wavelength range. The results of EQE measurements suggest that the hole limiting transport is responsible for the reduction of EQE with increasing N_s in long wavelength range in the case of p-side illumination and in entire wavelength range in the case of n-side illumination.

The effects of the spin density of the absorber layer on the performance of p-side and n-side illuminated solar cells were further investigated with computer simulations using the software package Advanced Semiconductor Analysis (ASA).¹³ The simulation parameters were taken from Ref. 14. The simulation parameters include the defect density, varied between $1.4 \times 10^{16} \text{ cm}^{-3}$ and $2.5 \times 10^{18} \text{ cm}^{-3}$. As only neutral defects contribute to the spin density, we need to relate a given spin-density to a defect density. For each measured spin-density, we iteratively determined the corresponding defect density such that the simulated concentration of neutral defects in a single intrinsic layer is equal to the measured spin-density. Note that the relation between the number of neutral defects and total defect density depends on several simulation parameters, such as the mean energy and width of the Gaussian distribution of defects. We find that in the simulations, the difference in carrier mobilities (we assumed 50

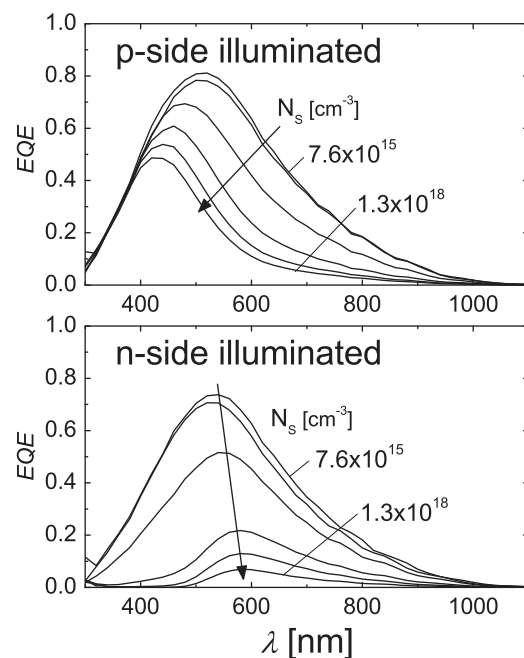


FIG. 2. Experimental EQE curves for p-side and n-side illuminated $\mu\text{c-Si:H}$ solar cells with varied N_s of the absorber layer. The spin density values N_s from top to bottom are: 7.6×10^{15} , 1.8×10^{16} , 2.3×10^{16} , 1.8×10^{17} , 3.4×10^{17} , and $1.3 \times 10^{18} \text{ cm}^{-3}$.

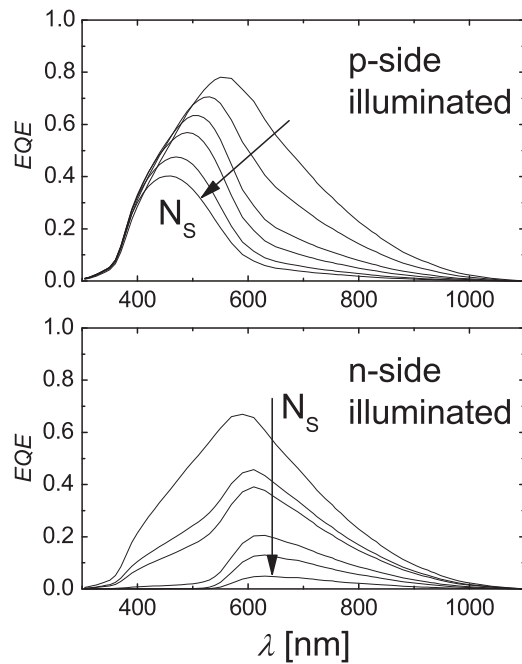


FIG. 3. Simulated EQE curves for p-side and n-side illuminated $\mu\text{c-Si:H}$ solar cells with varied N_s of the absorber layer. The sequence of spin density values N_s is the same as shown in Fig. 2.

and $15 \text{ cm}^2/\text{Vs}$ for electrons and holes, respectively) cannot explain the observed differences between p- and n-side illuminated devices. However, if we set the center of the Gaussian distribution of dangling bonds at 0.2 eV above mid-gap, we obtain a good agreement with experimental J - V curves and EQE measurements, as shown in Fig. 3. This shift in position of the dangling bonds is schematically illustrated in Fig. 4. Shifting the mean energy for the defect distribution to above mid gap makes the material slightly n-type. This in turn results in a higher electric field near the p-i interface at the expense of the electric field near the i-n interface.

Note that the reference parameter set from Ref. 14 was carefully calibrated using temperature dependent dark J - V -curves, illuminated J - V -curves and EQE measurements and, furthermore, is consistent with experimental data from a large body of literature. For this reason, we took care not to deviate too far from the reference parameter set. The only difference with the reference parameter set is a small change in the mean energy of the defect distribution and, of course, the defect density as it was varied in our experiments. For low defect densities, this shift in mean energy has virtually no influence on the results, i.e., for low defect densities, our parameter set is equivalent to the reference parameter set.

In summary, key differences in the performance for p-side and n-side illuminated $\mu\text{c-Si:H}$ solar cells are observed when the absorber layer defect density increases above $N_s = 3 \times 10^{16} \text{ cm}^{-3}$. Reduced performance of n-side illumi-

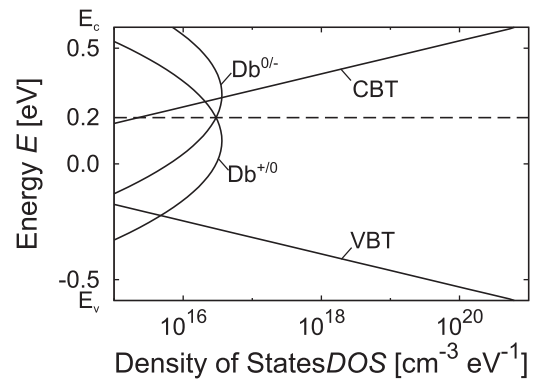


FIG. 4. Density of states used in the simulations for intrinsic $\mu\text{c-Si:H}$ with $N_s = 7.6 \times 10^{15} \text{ cm}^{-3}$. Shown are the distributions of valence band tail states (VBT), the conduction band tail states (CBT), and the distribution of amphoteric dangling bond states, where $\text{Db}^{0/+}$ represents the $+/0$ transition level and $\text{Db}^{0/-}$ the $0/-$ transition level. The center of the dangling bond distribution is located 0.2 eV above mid-gap (with mid gap at 0 eV).

nated cells (relative to p-side illuminated devices), particularly in J_{sc} , suggests that the high quality $\mu\text{c-Si:H}$ absorbers are necessary for improved performance. The results of computer simulation demonstrate that the observed asymmetry in performance can be explained by the assumption that the center of the Gaussian defect distribution is 0.2 eV above mid-gap.

We thank W. Böttler and W. Reetz for contributions to this work and U. Rau for continuous support and encouragement. Financial support of this work by the German Federal Ministry of Education and Research (BMBF network Project EPR-Solar 03SF0328) and by European Community (STCU Project #P429) is gratefully acknowledged.

- ¹J. P. Xi, Y. S. Tsuo, J. U. Trefny, and T. J. McMahon, in *Proceedings of the 18th IEEE Photovoltaic Specialists Conference* (1985), p. 519.
- ²M. Hack and M. Shur, *J. Appl. Phys.* **58**, 997 (1985).
- ³R. Schropp and M. Zeman, *Amorphous and Microcrystalline Silicon Solar Cells* (Kluwer Academic, Norwell, MA, 1998).
- ⁴A. Gross, O. Vetterl, A. Lambertz, F. Finger, H. Wagner, and A. Dasgupta, *Appl. Phys. Lett.* **79**, 2841 (2001).
- ⁵T. Dylla, F. Finger, and E. A. Schiff, *Appl. Phys. Lett.* **87**, 032103 (2005).
- ⁶Y. Huang, A. Dasgupta, A. Gordijn, F. Finger, and R. Carius, *Appl. Phys. Lett.* **90**, 203502 (2007).
- ⁷V. Smirnov, A. Lambertz, B. Grootenok, R. Carius, and F. Finger, *J. Non-Cryst. Solids* **358**, 1954 (2012).
- ⁸M. Kondo, *Sol. Energy Mater. Sol. Cells* **78**, 543 (2003).
- ⁹V. Smirnov, O. Astakhov, R. Carius, Yu. Petrusenko, V. Borysenko, and F. Finger, *Jpn. J. Appl. Phys.* **51**, 022301 (2012).
- ¹⁰O. Astakhov, V. Smirnov, R. Carius, Yu. Petrusenko, V. Borysenko, W. Böttler, and F. Finger, *J. Non-Cryst. Solids* **358**, 2198 (2012).
- ¹¹O. Astakhov, R. Carius, F. Finger, Yu. Petrusenko, V. Borysenko, and D. Barankov, *Phys. Rev. B* **79**, 104205 (2009).
- ¹²W. Böttler, V. Smirnov, A. Lambertz, J. Hüpkes, and F. Finger, *Phys. Status Solidi C* **7**, 1069 (2010).
- ¹³B. E. Pieters, J. Krc, and M. Zeman, in *2006 IEEE 4th WCPEC* (2006), p. 1513.
- ¹⁴B. E. Pieters, H. Stiebig, M. Zeman, and R. A. C. M. van Swaaij, *J. Appl. Phys.* **105**(4), 044502 (2009).